

Mesopores Cellular Foam-Based Electrochemical Sensor for Sensitive Determination of Ractopamine

Liping Xie¹, Yu Ya^{1,*} and Liang Wei^{2,*}

¹ Institute for Agricultural Product Quality Safety and Testing Technology, Guangxi Academy of Agricultural Sciences, Nanning 530007, China

² College of Chemistry and Materials Science, Guangxi Teachers Education University, Nanning 530001, China

*E-mail: yayu1026@163.com, weil@gxtc.edu.cn

Received: 26 June 2017 / Accepted: 5 August 2017 / Published: 12 September 2017

A mesopores cellular foam (MCF) modified carbon paste electrode (MCF/CPE) was designed for sensitive determination of ractopamine. The as-prepared MCF was characterized by scanning electron microscopy (SEM), transmission electron microscopy (TEM), X-ray diffraction (XRD), nitrogen adsorption-desorption isotherms and pore size distribution plots. Cyclic voltammetry (CV) and electrochemical impedance spectroscopy (EIS) were employed to demonstrate the large electrode surface and the fast electron transfer in the MCF/CPE which showed much better performance for the electrochemical oxidation of ractopamine when compared with the bare carbon paste electrode (CPE). Under optimized conditions, the oxidation peak current was proportional to the ractopamine concentration which was varied between 0.050 and 3.0 μM , with a detection limit (defined by a signal-to-noise ratio of three) of 0.010 μM . The proposed sensor was applied to determine the ractopamine content in pork samples with satisfactory results.

Keywords: Mesopores cellular foam, Modified electrode, Ractopamine, Linear sweep voltammetry

1. INTRODUCTION

Ractopamine belongs to β_2 -agonists and was originally developed for the treatment of pulmonary disease and asthma [1]. Meanwhile, it can improve the growth rate and reduce the carcass fat when used as feeding for animals [2]. Ractopamine is also used as a nutrient repartitioning agent in the livestock industry. However, ractopamine might be a potential danger for consumer health [3], and it is not licensed for animal production in many countries [4]. Hence, it is quite important to build a sensitive and accurate method for the detection of ractopamine.

Various techniques are now available for the determination of the ractopamine content, including chromatography [5-7], enzyme-linked immunosorbent assays [8-10], capillary electrophoresis [11-12], electrochemiluminescence [13-14] and electrochemical methods [15-22]. Electrochemical methods are a powerful tool for the determination of the ractopamine content thanks to advantages such as low-cost, operational simplicity, high sensitivity and fast response. More recently, nanomaterials have been employed in the electroanalysis of ractopamine due to the high surface area-to-volume ratio, high surface reaction activity and excellent electron transport properties [23-24]. Various types of nanomaterial modified electrodes were used for the detection of ractopamine, based on ordered mesoporous carbon [15], carbon nanotubes [16], poly taurine/zirconia nanoparticles [17], gold nanoparticles, multi-walled carbon nanotubes in a poly-arginine film [18], carbon nanoparticles [19] and flower-like gold nanostructure on ordered mesoporous carbon [20].

Mesopores cellular foam (MCF) is a novel new mesoporous silica material which has some similar properties as compared to the conventional ordered mesoporous materials such as high surface area and large pore volume. MCF is a three-dimensional (3D) material with ultra-large mesopores [25] with large pore size and 3D open mesostructure which is beneficial to the transport and diffusion of analytes in the channels. These properties make MCF an ideal candidate for electrochemical sensing [26-29]. Herein, a novel electrochemical sensor for ractopamine was fabricated by MCF-modified carbon paste electrode (MCF/CPE). The MCF/CPE exhibited excellent electrochemical properties and high sensitivity for the detection of ractopamine. In this work the MCF/CPE was successfully applied to detection of ractopamine in pork samples to demonstrate that it is a promising device for practical applications.

2. EXPERIMENTAL

2.1. Reagents and Instruments

The standard ractopamine was obtained from Sigma-Adrich (St. Louis, USA). Graphite powder (spectral reagent) and paraffin oil were purchased from Sinopharm Chemical Reagent Co., Ltd (Shanghai, China). MCF was prepared according to a previously reported method [30]. All other reagents were of analytical grade and were used as received. A phosphate buffer solution (PBS) was prepared from KOH and 0.1 M H_3PO_4 , and the pH was monitored using a pH meter. All aqueous solutions were prepared in deionized water.

Electrochemical measurements were conducted on a CHI660E electrochemical workstation (CH Instruments, Shanghai, China). A standard three-electrode cell was used for all electrochemical experiments with a bare or modified CPE ($d = 3.0$ mm) as the working electrode, a platinum wire was used as auxiliary electrode and a saturated calomel electrode (SCE) as the reference electrode. Transmission electron microscopy (TEM) images were obtained with a Tecnai G² F20 S-Twin microscope (FEI Ltd., USA). Scanning electron microscope (SEM) images were recorded on a Hitachi S-3400N microscope (Tokyo, Japan). X-ray diffraction (XRD) measurements were carried with a Bruker Advanced D8 diffraction instrument using Cu $K\alpha$ radiation (Karlsruhe, Germany). Surface area, pore size, and total pore volume of MCF were measured by using a Quantachrome Autosorb-1-C-MS instrument (Florida, USA). High-performance liquid chromatography determination of

ractopamine was carried out with a Waters 2695 liquid chromatograph coupled with an UV-vis detector (Milford, USA). pH values were measured using a Leici pH-3C precision pH meter (Shanghai, China).

2.2. Preparation of the working electrode

MCF/CPE was prepared by thoroughly mixing 0.0250 g of MCF with 1.0000 g of the graphite powder and 0.5 mL of paraffin oil. The mixing maintained until obtaining a homogenous wetted paste. In the absence of MCF, bare CPE was prepared using the same procedure. The resulting paste was tightly pressed into a polytetrafluoroethylene cylindrical tube ($d = 3.0$ mm) with a copper piston, providing an inner electrical contact. Then, the surface was polished on a smooth paper.

2.3. Sample preparation

Pork samples were purchased from a local supermarket and pretreated as follows [15-16]. Briefly, one gram of smashed sample was added to 4 mL 0.1 M HClO₄, ultrasonicated for 30 min, heated at 80 °C for 30 min and cooled at room temperature, the mixture was then separated by centrifugation at 5000 rpm for 10 min we collected the upper clear solution. The pH of obtained solution was adjusted to 10 by adding 10% Na₂CO₃, after that, 1.6 g NaCl were added to the solution. Subsequently, ractopamine was extracted twice using 10 mL ethyl acetate. The extracted solution was collected and evaporated in nearly dry conditions using a mild nitrogen stream. The residue was diluted to 10 mL using pH 8.5 PBS. Spiked samples were prepared by adding a known amount of ractopamine standard before treatment.

2.4. Electrochemical Measurement Procedures

Unless otherwise stated, electrochemical measurements were conducted in a conventional electrochemical cell containing 10 mL of 0.1 M PBS with a pH of 8.5, containing a certain concentration of ractopamine. After open circuit accumulation for 300 s under stirring, linear sweep voltammograms were recorded, the potential was scanned from 0 to 0.80 V with scan rate of 100 mV s⁻¹, then, the peak currents measured at 0.46 V were employed for determination of the ractopamine content.

3. RESULTS AND DISCUSSION

3.1. Characterization of MCF

The 3D mesoporous structure of MCF was investigated by electron microscopy. TEM images (Figure1A) of the MCF show a uniform 3D mesoporous structure. The mesoporous structure of MCF was further verified in SEM images (Figure1B).

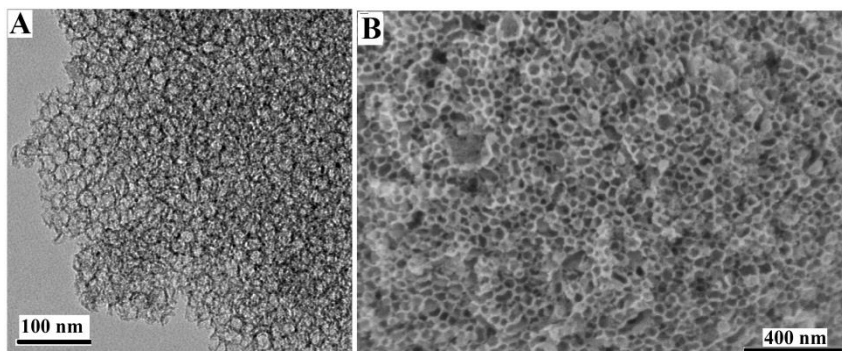


Figure 1. TEM (A) and SEM (B) images of MCF.

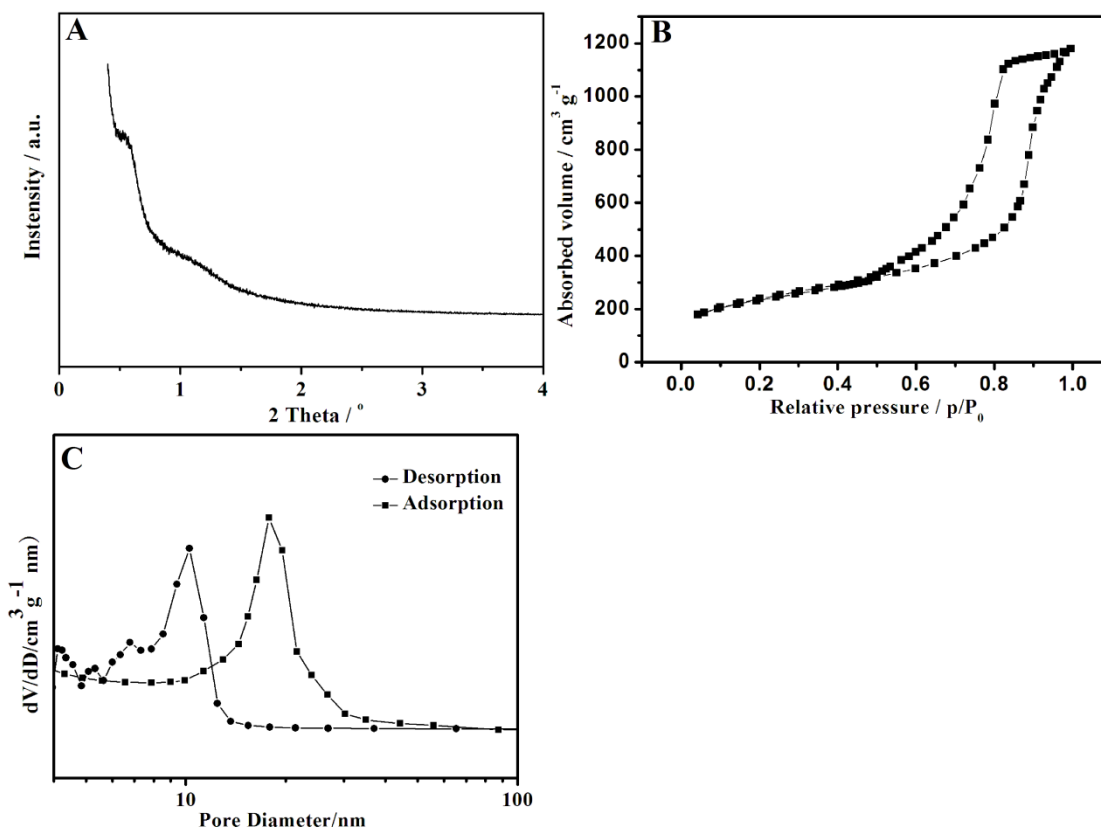


Figure 2. XRD pattern (A), nitrogen adsorption–desorption isotherms (B) and pore size distribution (C) of MCF.

The MCF structure was further investigated by small-angle XRD. As shown in Figure 2A, a diffraction peak was observed between 0.5° and 1° indicating that the size distribution of the 3D spherical pores is relatively narrow [30]. Nitrogen adsorption–desorption isotherms of MCF are shown in Figure 2B. For a typical mesoporous structure, isotherms clearly show a type IV behavior with type H1 hysteresis loops [30–31]. The surface area and the pore volume of MCF calculated from isotherms using the Brunauer–Emmett–Teller (BET) method, indicate a BET surface area of $782.8 \text{ m}^2\text{g}^{-1}$ and the pore volume of $1.83 \text{ m}^3\text{g}^{-1}$. The pore size distribution can be calculated from the adsorption and desorption branches of the isotherms using the Barrett–Joyner–Halenda (BJH) method. Figure 2C

shows a double pore size distribution in MCF with large cell pores interconnected with uniform window pores. The pore size distribution plots are centered at 10 and 18 nm, thus we conclude that the MCF is composed of main cells with a diameter of 18 nm interconnected by 10 nm windows [29].

3.2. Electrochemical characterization of the modified electrode

$[\text{Fe}(\text{CN})_6]^{3-/4-}$ was employed as a probe to investigate the electrochemical properties of the MCF/CPE electrode. Figure 3A shows cyclic voltammograms of 5.0 mM $[\text{Fe}(\text{CN})_6]^{3-/4-}$ for the bare CPE (curve a) and the MCF/CPE (curve b). The peak-to-peak separation (ΔE_p) of $[\text{Fe}(\text{CN})_6]^{3-/4-}$ probe is 168 mV for the bare CPE and it decreases to 114 mV for the MCF/CPE. In addition, the response current of the probe increased significantly in the MCF/CPE. It can be deduced that the presence of MCF significantly accelerates the electron transfer between the probe and the modified electrode. The electroactive area was calculated from the Randles–Sevcik equation [15]:

$$I_p = 2.69 \times 10^5 D^{1/2} n^{3/2} A \nu^{1/2} C \quad (1)$$

where I_p refers to the peak current (μA), D is the diffusion coefficient ($\text{cm}^2 \text{s}^{-1}$), n is the electron-transfer number, A is the electroactive surface area of the electrode (cm^2), ν is the scan rate (V s^{-1}), and C is the concentration of $[\text{Fe}(\text{CN})_6]^{3-/4-}$ (mM). Here, $D = 0.76 \times 10^{-5}$, $n = 1$, $\nu = 0.1$, and $C = 5.0$. The electroactive area of the bare CPE and the MCF/CPE results 0.0394 and 0.0607 cm^2 , respectively, indicating that MCF can be effectively improve the electroactive area of the electrode surface.

The EIS was employed to further investigate the charge transfer resistance of bare CPE and MCF/CPE (Figure 3B). A clear semicircle is observed on the bare CPE, while the MCF/GCE exhibits a nearly straight line. The EIS results thus further confirm that the MCF modification can significantly improve the electrochemical properties of electrode.

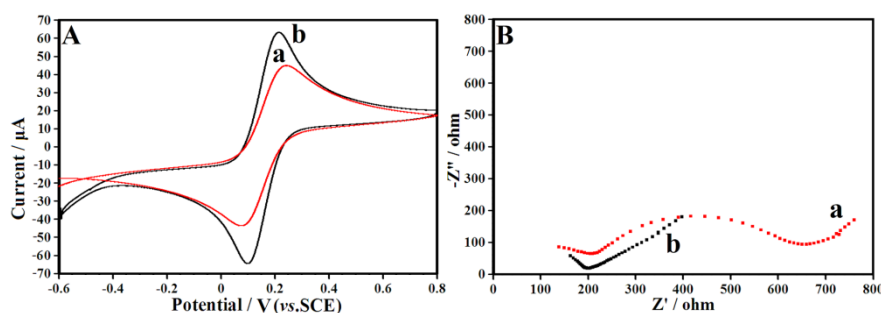


Figure 3. Cyclic voltammetry curves (A) and Nyquist plots of EIS (B) of bare CPE (a) and MCF/CPE (b) measured in 5.0 mM $[\text{Fe}(\text{CN})_6]^{3-/4-}$.

3.3. Electrochemical oxidation of ractopamine

The electrochemical behavior versus ractopamine detection was studied using cyclic voltammetry (CV). Figure 4 shows the CV curves for 0.50 μM ractopamine content obtained with the bare CPE (curve a) and the MCF/CPE (curve b). Only one anodic peak is obtained with both electrodes demonstrating a totally irreversible electrode reaction with ractopamine. With MCF the

peak potential is shifted negatively and the peak current is obviously increased, testifying a strong enhancement of the electrochemical oxidation of ractopamine. The strong enhancement effect induced by the MCF was attributed to two factors: the first is the presence of 3D open pore channels which are beneficial to the diffusion of ractopamine through the pores, at the same time, the large surface area allow increasing the loading amount of ractopamine in the cavities of MCF. The second is the excellent conductivity of the MCF matrix, which acts as an electron transfer tunnel, thereby favoring electron transfer between ractopamine and the electrode [28-29].

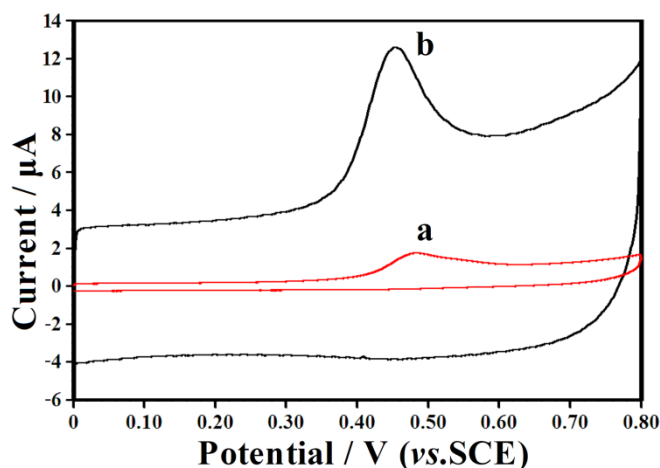


Figure 4. CV curves for 0.50 μM ractopamine content at pH 8.5 PBS for the bare CPE (a) and MCF/CPE (b).

Linear sweep voltammetry (LSV) was used to study the effect of the scan rate on the electrochemical oxidation of ractopamine. Superimposed voltammograms for 0.50 μM ractopamine with the scan rate (ν) ranging from 0.025 to 0.300 V s^{-1} are shown in Figure 5A. The oxidation peak current result to increase linearly with the square root of scan rate; the regression equation was: $i_p = -2.182 + 27.94 \nu^{1/2}$ (V s^{-1}) ($R = 0.997$), indicated that electrochemical oxidation of ractopamine occurring at the MCF/CPE electrode was a diffusion-controlled process. Additionally, the peak potential (E_p) shifted positively when increasing ν . As shown in Figure 5B, a fairly linear relationship resulted between E_p and $\ln \nu$ with regression equation: E_p (V) = 0.5399 + 0.03176 $\ln \nu$ (V s^{-1}) ($R = 0.998$). According to Laviron's theory, in an irreversible electrode process, the $E_p - \ln \nu$ relation can be described by the following equation [32]:

$$E_p = E^0 - \frac{RT}{\alpha n F} \ln \nu \quad (2)$$

where E^0 is the formal standard potential (V), R is the universal gas constant (8.314 J/mol K), T is the temperature (298 K), α is the electron-transfer coefficient, n is the electron-transfer number and F is the Faraday constant (96,480 C/mol). In this study, αn is calculated to be 0.8086. For a totally irreversible electrode process, α usually takes values between 0.4 and 0.6 [15]. We deduce that two electrons are involved in the electrochemical oxidation of ractopamine.

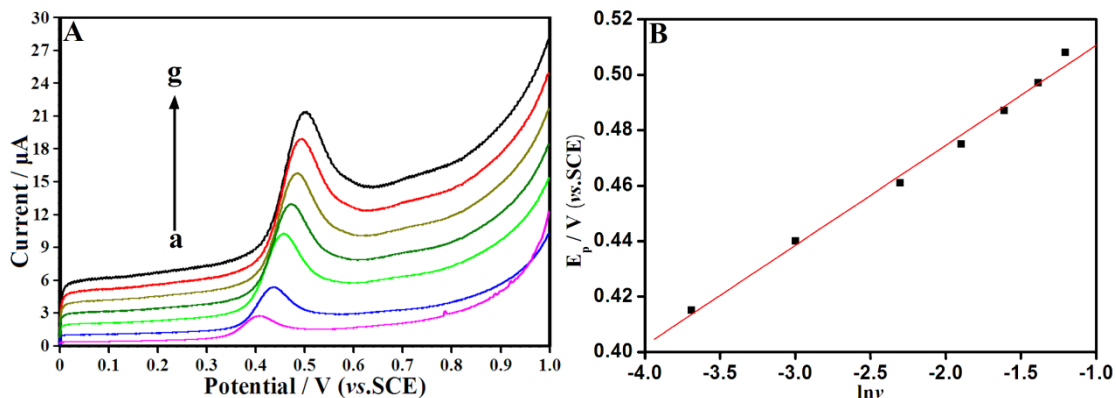


Figure 5. (A) LSV curves obtained for a ractopamine content of 0.50 μM with the MCF/CPE at pH 8.5 (PBS) for different scan rate (from a to g: 0.025, 0.050, 0.10, 0.15, 0.20, 0.25 and 0.30 V s⁻¹). (B) The plot of E_p of ractopamine versus the logarithm of scan rate.

3.4. Effect of the pH and the accumulation time

Figure 6A displays the influence of the pH on the peak current and E_p in the presence of 0.50 μM ractopamine concentration. The peak current increases when increasing the pH from 5.0 and 8.5 and then decreases for higher pH values. To maximize the sensitivity for the detection of ractopamine, the pH 8.5 PBS was selected. Furthermore, the E_p linearly shifted negatively with the increasing of pH value, suggesting that protons directly participate in the electrochemical oxidation of ractopamine. The linear regression equation was: $E_p = 0.9950 - 0.06475 \text{ pH}$ ($R = 0.999$), The slope value of 64.75 mV/pH was close to the theoretical value of -59.0 mV/pH, indicating that the number of electron transferred was equal to the number proton involved in the electrochemical oxidation of ractopamine. Therefore, the oxidation of ractopamine involves two protons and two electrons, which is in agreement with previous literature reports [15-16].

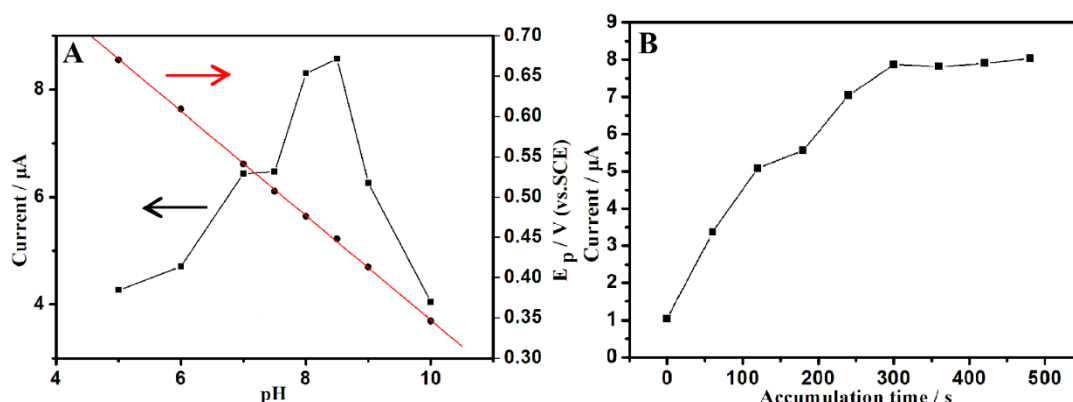


Figure 6. (A) Effect of pH on the peak current and E_p at the MCF/CPE for a ractopamine content of 0.50 μM. (B) Effect of accumulation time on the peak current in the same conditions.

The influence of the accumulation time on the peak current for 0.50 μM ractopamine content was investigated in the range between 0 to 480 s (Figure 6B). By extending the accumulation time from 0

to 300 s, the peak current increased significantly. A further increase of the accumulation time, lead only to a slight enhancement of the oxidation peak current, suggesting that the amount of ractopamine on the surface of MCF/CPE tended to be saturated. By taking both the sensitivity and the efficiency in consideration, an accumulation time of 300 s was chosen for the further experiments.

3.5. Voltammetric determination of ractopamine

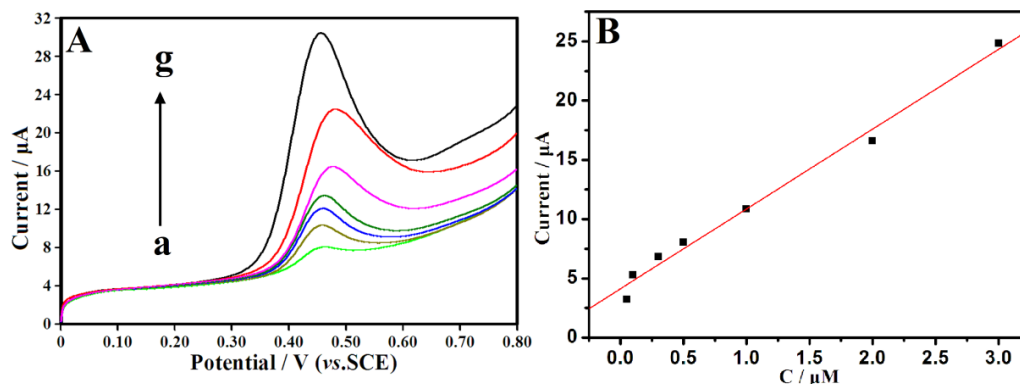


Figure 7. (A) LSV curves obtained at pH 8.5 with the MCF/CPE for different ractopamine concentrations (from a to g: 0.050, 0.10, 0.30, 0.50, 1.0, 2.0 and 3.0 μM). (B) Linear relationship between the current response and the ractopamine concentration.

Table 1. Comparison of the proposed sensor with other sensors for ractopamine detection

Modified electrode	Linear range (μM)	Detection limit (μM)	Reference
Ordered mesoporous carbon modified electrode	0.085 - 8.0	0.060	15
Carbon nanotube film-modified electrode	0.15 - 5.9	0.059	16
Poly taurine/zirconia nanoparticles modified electrode	1.0 - 28	0.15	17
Electrode modified with gold nanoparticles and multi-walled carbon nanotubes in a poly-arginine film	0.00010 - 1.0	0.00010	18
Carbon nanoparticle modified electrode	0.0020 - 0.030	0.0020	19
Flower-like gold nanostructure on ordered mesoporous carbon electrode	0.030 - 75	0.0044	20
Arrays of micro-liquid / liquid interfaces	0.10 - 1.0	0.10	21
Molecular imprinted membrane assemble on screen-printed electrode modified with ordered mesoporous carbon and gold nanoparticles	0.000050 - 0.0010	0.000042	22
MCF/CPE	0.050 - 3.0	0.010	This work

The linear range and detection limit were tested using LSV under the optimized conditions. Figure 7A shows the superimposed LSV curves obtained for different ractopamine concentrations in the range between 0.050 and 3.0 μM . As shown in Figure 7B, the peak current was proportional to the ractopamine concentration, with a good correlation ($R = 0.995$). The linear regression equation was i_p (μA) = 4.162 + 6.713 C (μM), and the detection limit was 0.010 μM (signal-to-noise ratio = 3). Moreover, MCF/CPE exhibited good reproducibility with a relative standard deviation (RSD) of 5.22% for 5 individual measurements. The stability of the MCF/CPE was investigated after long-term storage in air for one week, showing that 95.8% of the original oxidation peak current was retained. From these results, it is evident that the MCF/CPE exhibits both good reproducibility and stability.

Moreover, a comparison of analytical performance of MCF/CPE with other ractopamine sensors has been made and given in Table 1. As we can see, the MCF/CPE shows good analytical properties for the electrochemical detection of ractopamine.

Potential interferences for the detection of 0.50 μM ractopamine content were investigated under the optimized conditions. The tolerance limit was defined as the maximum concentration of the interfering species that caused a detection error less than $\pm 5.0\%$. It was found that 1000-fold Na^+ , K^+ , Ca^{2+} , Mg^{2+} , Cu^{2+} , Zn^{2+} , Fe^{3+} , Al^{3+} , Cl^- , NO_3^- , CO_3^{2-} , SO_4^{2-} , glucose and sucrose; 200-fold uric acid, ascorbic acid, amidopurine and guanine; 100-fold dopamine; 80-fold clenbuterol, had no influence on the signal of the 0.50 μM ractopamine.

3.6. Detection of ractopamine in pork samples

To evaluate the feasibility of the developed method, the MCF/CPE was applied for the evaluation of the ractopamine content in commercial pork samples by using a standard addition method. The sample treatment is described in section 2.3. No ractopamine was detected in two pork samples. Results obtained in spiked samples are summarized in Table 2. The value of recovery is in the range from 88.9% to 98.3%. Meanwhile, the electrochemical results were coincident with that of HPLC detection [5]. This implies that the developed method is both accurate and feasible.

Table 2. Results for the determination of ractopamine in porks samples

Sample	Spiked ($\mu\text{g g}^{-1}$)	Found ($\mu\text{g g}^{-1}$)	Recovery (%)	By HPLC ($\mu\text{g g}^{-1}$)
A	1.35	1.20	88.9	1.26
	2.70	2.48	91.8	2.61
	5.40	5.31	98.3	5.62
B	1.35	1.24	91.8	1.22
	2.70	2.58	95.6	2.82
	5.40	5.08	94.1	5.12

4. CONCLUSION

In this work, we have designed a highly sensitive electrochemical sensor for the detection of ractopamine based on the MCF/CPE which exhibited excellent electrochemical properties. These properties were ascribed to the large electroactive area and its 3D open mesostructure. As an advanced sensor electrode, the MCF/CPE is expected to have promising future applications in the electroanalytical field.

ACKNOWLEDGEMENTS

The authors gratefully acknowledge the financial support by the science and technology development fund of Guangxi Academy of Agricultural Sciences (No. 2017JZ39, 2017JM57 and 2015YT94) as well as “BAGUI Scholar Program” of Guangxi Province of China.

References

1. G.H. Loneragan, D.U. Thomson and H. M. Scott, *Plos One*, 9 (2014) e91177.
2. M.J. Yaeger, K. Mullin and S.M. Ensley, *Vet. Pathol.*, 49 (2012) 569.
3. W.C. Chen, Y.C. Wang, J.L. Shen, H.Y. Chen, C.H. Chang, F.J. Tsai, W.Y. Lin and Y.H. Chen, *J. Food Nutr. Res.*, 3 (2015) 670.
4. T. Peng, A.L. Royer, Y. Guitton, B.L. Bizec and G. Dervilly-Pinel, *Metabolomics* 13 (2017) 77.
5. K. Yan, H. Zhang, W. Hui, H. Zhu, X. Li, F. Zhong, X. Tong and C. Chen, *J. Food Drug Anal.*, 24 (2016) 277.
6. V.G. Amelin, D.S. Korolev and A.V. Tret'yakov, *J. Anal. Chem.*, 70 (2015) 419.
7. A.V. Vales, G.A.P. Oliveira, C.R. Kleemann, L. Molognoni and H. Daguer, *J. Food Compos. Anal.*, 47 (2016) 38.
8. A. Liu, J. Lin, M. Dai, B. Ma, Y. Wu, J. Fang and M. Zhang, *Food Anal. Methods*, 9 (2016) 2016.
9. S. Wang, S. Zhao, X. Wei, S. Zhang, J. Liu and Y. Dong, *Sensors*, 17 (2017) 604.
10. J. Liang, H. Liu, C. Huang, C. Yao, Q. Fu, X. Liu, D. Cao, Z. Luo and Y. Tang, *Anal. Chem.*, 87 (2015) 5790.
11. W. Wang, Y. Zhang, J. Wang, X. Shi, and J. Ye, *Meat Sci.*, 85 (2010) 302.
12. T.A.H. Nguyen, T.N.M. Pham, T.T. Doan, T.T. Ta, J. Sáiz, T.Q.H. Nguyen, P.C. Hauser and T.D. Mai, *J. Chromtogr. A*, 1360 (2014) 305.
13. S. Wang, J. Wei, T.T. Hao and Z. Guo, *J. Electroanal. Chem.*, 664 (2012) 146.
14. Q. Zhu, H. Liu, J. Zhang, K. Wu, A. Deng and J. Li, *Sens. Actuators, B*, 243 (2017) 121.
15. X. Yang, B. Feng, P. Yang, Y. Ding, Y. Chen and J. Fei, *Food Chem.*, 145 (2014) 619.
16. Z. Liu, Y. Zhou, Y. Wang, Q. Chen and K. Wu, *Electrochim. Acta*, 74 (2012) 139.
17. M. Rajkumar, Y.S. Li and S.M. Chen, *Colloids Surf. B*, 110 (2013) 242.
18. Y. Zhou, P. Wang, X. Su, H. Zhao and Y. He, *Microchim. Acta*, 181 (2014) 1973.
19. S. Yao, Y. Hu, G. Li and Y. Zhang, *Electrochim. Acta*, 77 (2012) 83.
20. Q. Wei, Q. Wang, H. Wang, H. Gu, Q. Zhang, X. Gao and B. Qi, *Mater. Lett.*, 147 (2015) 58.
21. M. Sairi and D.W.M. Arrigan, *Talanta*, 132 (2015) 205.
22. M. Ma, P. Zhu, F. Pi, J. Ji and X. Sun, *J. Electroanal. Chem.*, 775 (2016) 171.
23. S. Campuzano and J. Wang, *Electroanal.*, 23 (2011) 1289.
24. N. Yang, G.M. Swain and X. Jiang, *Electroanal.*, 28 (2016) 27.
25. P. Schmidt-Winke, W.W.L. Jr, P. Yang, D.I. Margolese, J.S. Lettow, J.Y. Ying and G.D. Stucky, *Chem. Mater.*, 12 (2000) 686.
26. L. Zhang, Q. Zhang and J. Li, *Biosens. Bioelectron.*, 26 (2010) 846.

27. M.K. Bojdi, M. Behbahani, F. Omid and G. Hesam, *New J. Chem.*, 40 (2016) 1519.
28. Z. Xue, C. Hu, H. Rao, X. Wang, X. Zhou, X. Liu and X. Lu, *Anal. Methods*, 7 (2015) 1167.
29. S. Wu, H. Ju and Y. Liu, *Adv. Funct. Mater.*, 17 (2007) 585.
30. L. Wei, Y. Zhao, Y. Zhang, C. Liu, J. Hong, H. Xiong and J. Li, *J. Catal.*, 340 (2016) 205.
31. W. Zhu, Y. Han and L. An, *Micropor. Mesopor. Mat.*, 72 (2004) 137.
32. E. Laviron, *J. Electroanal. Chem.*, 52 (1974) 355.

© 2017 The Authors. Published by ESG (www.electrochemsci.org). This article is an open access article distributed under the terms and conditions of the Creative Commons Attribution license (<http://creativecommons.org/licenses/by/4.0/>).